

BEHAVIOR OF GEOGRID-PILE FOUNDATION SYSTEM IN LOOSE SANDY SOILS UNDER HALABJAH EARTHQUAKE

*Athraa Abdul Ameer Sadiq Al Ghanim¹, Qassun Saad Mohammed Shafiqu², Asma Thamir Ibraheem³

^{1,2,3} Civil Engineering Department, Al-Nahrain University, Baghdad, Iraq

*Corresponding Author, Received: 18 July 2019, Revised: 04 Sept. 2019, Accepted: 26 Oct. 2019

ABSTRACT: Due to the increase in seismic activity in Iraq recently and the need to reduce the damage to the foundations, this research has been carried out in order to study the response of the pile foundation reinforced by geogrid in loose sandy soils. Because of the paucity of information linking the pile foundations with geogrid, the geogrid used in this research to reinforce the loose sandy soil under earthquake loading. Three types of geogrid are used in loose sand under the influence of the largest wave of earthquakes hit the regions of Iraq zones known Halabjah earthquake. Results predict the impact of treatment on the piles, and to study the settlement, horizontal displacements and bending moment of the piles, as well as the accelerations and pore water pressure of the soil. It was concluded that adding geogrid to the pile foundation would be reduced settlement, horizontal displacement, tip load and bending moment of the pile.

Keywords: Acceleration, Bending moment, Earthquake, Geogrid, Loose sand, Pile, Shaking table, Strain gauge.

1. INTRODUCTION

There was a need to find solutions to eliminate the damage of earthquakes on the deep foundations under dynamic effects Taha [1] and Zanzinger et al. [2], which has used the geogrid mesh with the pile foundation in the soft soil to reduce the settlement or enhance the lateral performance of piles under the effect of dynamic loads. Because of the lack of researches that uses the real waves with sandy soils for study such subject, Halabjah earthquake is one of the strong earthquakes that hit Iraq regions in 2017 that used in the experimental work. The experimental part includes constructing laboratory models, which include spread the geogrid inside the loose sandy soil and connect it with the piles using special connections designed for this purpose (rings). 18 tests were performed using shaking table manufactured by Al-Tameemi [3] and Al-Sammaray [4]. In the current research, the geogrids used are Tensar SS2, Netlon CE121, and SQ12. 7 tests carried on single pile in dry sandy soil, 3 tests are performed on single pile in saturated sand and 8 tests of 2 and 4 piles in dry sand.

2. MATERIAL AND INSTRUMENTS USED

2.1 The Sand Used

The curve of the particle size distribution for backfill material is shown in Fig.1. The soil is classified as poorly graded sand (SP) according to the Unified Soil Classification System USCS the tests for physical and chemical properties of sand were carried out under standard specifications of ASTM and BS respectively. The physical and chemical properties of sand used were listed in Table 1.

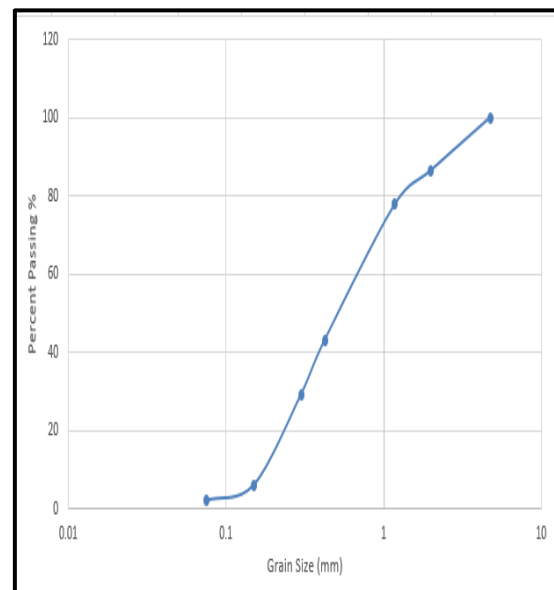


Fig.1. The particle size distribution

2.2 The Geogrid Reinforcement

Three types of geogrid are used, Tensar SS2, Nelton CE121 and SQ12 geogrids. The physical properties of geogrid used in this study listed in Table2 according to Fakhraldin [5]. The geogrid spread within the sand soil layer with dimensions 200×200 mm and 700×700 mm at the depth equal to L/8 (where L is the embedded pile length). The geogrid mesh connected to model piles by the rings, that is made of polytetrafluoroethylene (PTFE) which known as

Teflon and is similar to that used by Taha [6-7]. Four rings fabricated and installed to facilitate the load transfer between piles and the geogrid. The geogrid mesh extended and pressed inside the ring using four steel bolts. Rings fixed in their vertical position using a steel bolt as shown in Fig 2.

Table 1 The physical and Chemical properties of sand

| Soil Property | Units | Value | Standard |
|---|----------------------|------------------------|------------|
| Max. Unit Weight, γ_{max} | (kN/m ³) | 17.77 | ASTM-D4253 |
| Min. Unit Weight, γ_{min} | (kN/m ³) | 13.962 | ASTM-D4254 |
| Dry Unit Weight, γ_d | (kN/m ³) | 15.25 | - |
| Total Unit Weight, γ_t | (kN/m ³) | 17.16 | - |
| Water Content, W_c | % | 24 | ASTM-D2216 |
| Specific Gravity, G_s | - | 2.60 | ASTM-D854 |
| Max. Void Ratio, e_{max} | - | 0.827 | - |
| Min. Void Ratio, e_{min} | - | 0.434 | - |
| Effective Size, D_{10} | (mm) | 0.18 | - |
| Mean Size, D_{30} | (mm) | 0.30 | ASTM-D422 |
| Mean Size, D_{60} | (mm) | 0.7 | - |
| Permeability Coefficient ¹ , k | (cm/sec) | 2.461×10^{-3} | ASTM-D2434 |
| Friction Angle, ϕ | ° | 33° | ASTM-D4767 |
| SO_3 , | % | 2.6 | - |
| Gypsun content, | % | 5.59 | BS-1377 |
| T.S.S. | % | 0.74 | - |

2.3 The Piles

The piles used are made of an Aluminum bar. The Aluminum bar has a thickness of 1.4 mm and 16 mm diameter. The length to diameter ratio (L/D) is 25. Aluminum material used due to its lower modulus of elasticity and better thermal self-compensation effect to reduce the error caused by temperature variation.

Table 2 Specification of geogrid

| Type of geogrid | Unit | Nelton CE121 | SQ12 | Tensar SS2 |
|-----------------------------------|-------------------|--------------|--------|------------|
| Mesh type | - | Diamond | square | Rectangle |
| color | - | black | green | /black |
| Aperture size(MD/X MD) | mm | 6×8 | 12×12 | 28/40 |
| Mass per unit area | Kg/m ² | 0.740 | 0.318 | 0.3 |
| Rib thickness | mm | 1.6/1.45 | 1.7 | 1.2/1.1 |
| Junction thickness | mm | 2.75 | 1.6 | 3.9 |
| Peak tensile resistance | kN/m | 6.4 | 0.25 | 14.4/28.2 |
| Elastic modulus | MPa | 390 | 280 | 570/990 |
| Tensile strength | MPa | 9 | 2 | 24/30.7 |
| Percentage elongation at max load | % | 6 | 1 | 3.5/2.9 |
| Upper yield strength | MPa | 5 | - | 1/3 |

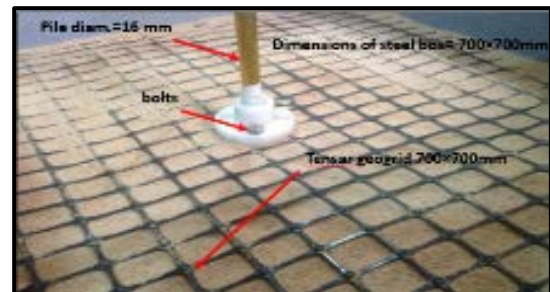
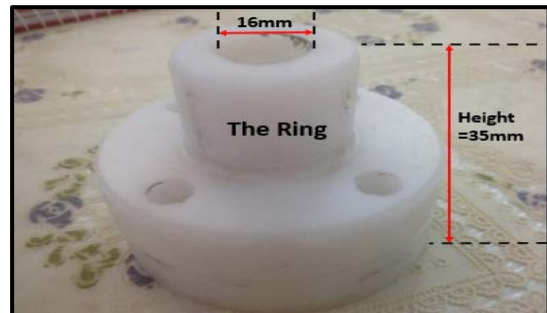


Fig 2a-b. Rings, mesh geogrid and the connections

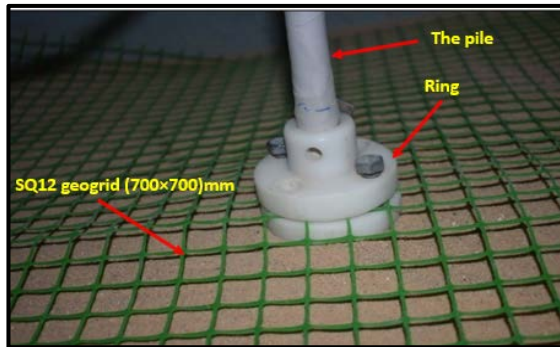
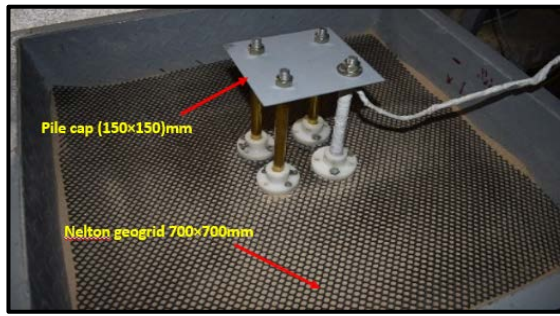


Fig 2c-d. Rings, mesh geogrid and the connections

The tension test was performed on the Aluminum bar to determine its strength and elastic modulus, the mechanical properties are listed in Table 3. The arrangement of piles used in this study is a single pile and [1x2] and [2x2] pile groups with distance between piles of 5D (D is the diameter of pile). The embedded length of pile is 400 mm. The sensors installed on the piles to measure the bending moment, the tip load and the displacements in three directions. These sensors are strain gauges, mini-load cell and displacement transducers. Install three strain gauges at the head, mid-length and at the end of the embedded pile for single and group piles tested in dry and saturated soil as shown in Fig.3. The wires of strain gauges passed inside the pile and it covered with waterproof past to avoid damage. Mini load cell (LCI) type "YGX601L-13" mounted at the bottom of the pile with a diameter of 16 mm and a capacity of 0.5 kN. The displacement transducers type (JX-PA-50-N11-21S-31N) mounted at the pile head to measure the displacement in three directions. Special waterproof used to protect strain gauges and availability skin friction for the pile. The piles are connected using pile cap made of steel material with dimensions 150× 150 mm as shown in Fig.2.



(a) Locations of strain gauges and load cell on the pile



(b) waterproof around the pile

Fig.3. The pile used and its sensors

Table 3 Mechanical properties of the tested pile

| Mechanical properties | Unit | Data |
|-----------------------------|-------------------|-------|
| Length of the embedded pile | mm | 400 |
| diameter | mm | 16 |
| Wall thickness | mm | 1.4 |
| Bending Stiffness $E_p I_p$ | kN.m ² | 0.116 |
| Unit Weight | kN/m ³ | 26.5 |
| Elastic modulus | GPa | 67 |
| Maximum load | kN | 14.23 |
| Max Elastic Stress | MPa | 221.6 |
| Maximum test elongation | % | 13.11 |

2.4 Instruments

Four accelerometers type (GY-61 ADXL335 3-axis) are used; three of them are placed in three different depths of the soil while the fourth placed on the table of shaking. Accelerometer covered with silicon and plastic for protecting them in saturated cases. Mini Pore water pressure manufactured by Tokyo Sokki Kenkyujo Co. Ltd, Japan placed in three depths of the saturated soil in the zone between the pile and the edge of steel container.

3. TEST PREPARATION

To prepare the system, the steel tank (700×700×800 mm) installed with the shaking table device using four screws, two spigots welded in adjacent faces of the steel tank, one for saturate the soil and another to discharge it through connected it with water pump to drain water from the soil after the test was finish. The water distribution system consists of panel PVC that was 19 mm diameter pipes constructed as square net pipes perforated. A constant head tank, which manufactured for this research to provide water in constant pressure to simulate groundwater table. Filter layer of thickness 150 mm placed in the bottom of steel box, which consists of graded coarse sand to prevent the soil from dragging with water when it is drained from the soil as shown in Fig.4-d. The water table was raised slowly from the base, this raising lead to escape of air to the surface layer gradually to ensure fully saturated condition. The steel box filled with sand by raining technique in layers, the device manufactured from steel tank, with dimensions 600mm length, 400mm width and 250mm height, provided with eight mechanical gates located at the base of steel box with dimensions of 600 mm length, 50mm width and 3mm thickness as shown in Fig4-e. These gates opened manually and joined with axial shaft and lever to generate stream of sand, which flows through. The surface of the soil was leveled using level surface. The steel box is hanging to the ceiling by roller (2 tons) to the required depth, the relative density (D_r) of loose sand reach to 30%. ACC3 and PPT3 placed at 350 mm from the internal edge of the steel box. The single pile placed in the middle of the steel box at 350 mm from the inner edge of the tank. The pile group placed in the center of the steel box corresponding to the center of the pile cap. ACC2, PPT2 placed in the middle distance of the embedded pile while ACC1, PPT1 placed at depth $L/8$ from the surface of the soil. The geogrid was laid within the sand at depth $L/8$ and connect with the piles using the rings to prevent any slip between them. The cap was placed at depth of 150 mm above the surface level then loaded with allowable bearing capacity of single pile calculated by Hansen [8] which is equal to 0.0365 kN for single pile and multiplied with number of pile for group. After saturation, a program of

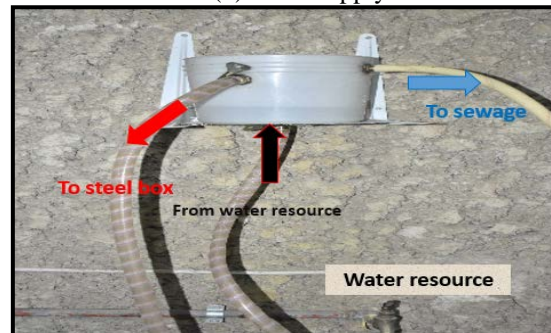
the Earthquake Simulator Software run, Halabjah earthquake selected, and then reset all sensors, then test started and the shake triggered while data from sensors streamed to the DAQ until the shaking ended. Later, data logged then analyzed by the software and test reports created.



(a) water distribution panel



(b) water supply



(c) water tank



(d) Filter material



(e) the raining technique
Fig.4. Saturation system and the raining technique

4. RESULTS

Figure 5 show the sketch of the geogrid-pile foundation system and the locations of a sensor, different sensors were used, three strain gauges were mounted on the pile to evaluate the bending moment, three displacement transducers were installed at the pile head to measure the settlement and the horizontal displacement in two directions. A miniature load cell type "YGX601L-13" was used with a maximum capacity of 0.5 kN. A mini load cell was fixed inside the pile tip to measure the end bearing capacity. Three accelerometer and pore pressure transducers sensors were placed at different depth as shown in Fig.5 to measure the acceleration and pore water pressure of the soil.

Table 4 Show the information of Halabjah earthquake used in the research.

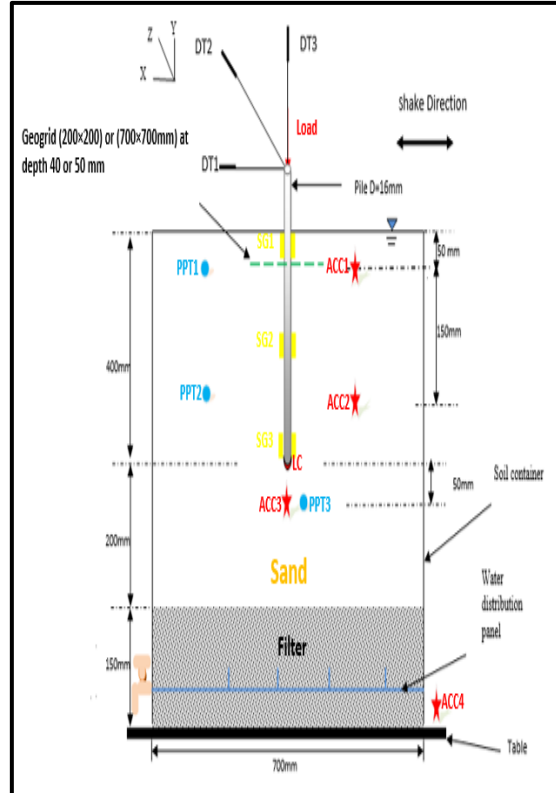


Fig.5. Sketch of laboratory test model

Table 4 Halabjah earthquake data

| Earthquake | Halabjah |
|-------------------------------------|--|
| Region | Iraq – Iran border |
| Data (UTC*) | 12/11/2017 18:18:17 |
| Magnitude, (M _w) | 7.3 M _w |
| Modified Mercalli Intensity, (MMI) | VIII- Moderated heavy |
| Epicenter depth, (Km) | 19 |
| Shake Duration, (sec) | 300 |
| Station distance to epicenter, (Km) | 218.8 |
| Sampling frequency,(Hz) | 10 |
| Acceleration direction | E-W |
| Maximum acceleration, (g) | 0.1 |
| Station code | BHD |
| Reference | Iraqi Meteorological Organization and Seismology |

Figure 6 illustrates the acceleration with dynamic time which has been inserted into the shaking table.

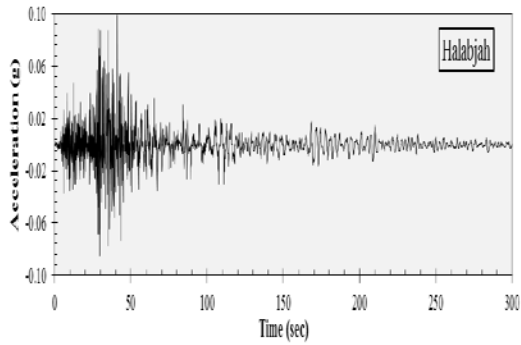


Fig.6. Acceleration with time for Halabjah earthquake

Figure 7 shows the maximum bending moment recorded by strain gauges with the embedded pile length. It was found that the maximum bending moment of the pile in the absence and presence geogrid would be near the surface and then gradually decreases in the lateral directions to the minimum bending moment at the end tip of the pile. This occurs because two reasons, the first one is settlement of soil surface, which caused due to shaking, and the second reason is the move away of the soil around the strain gauges at these locations. It was found that adding Nelton geogrid with dimensions 700×700mm would reduce the bending moment ratio (the difference between maximum bending moment without and with geogrid to the maximum bending moment without using geogrid) to about 12.5%, 20% and 80% along the pile length respectively.

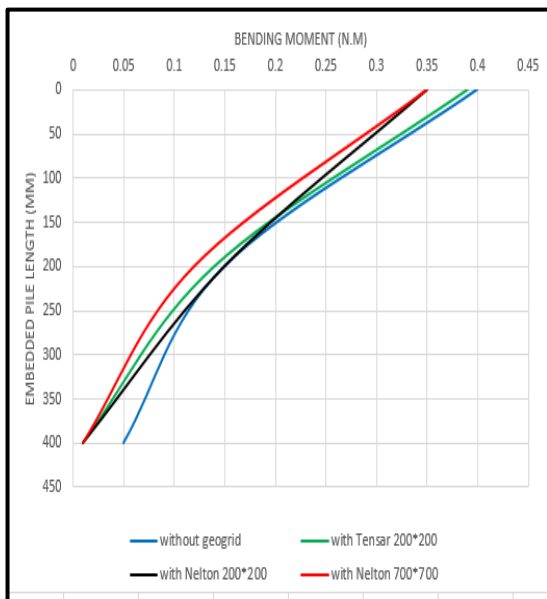


Fig.7. Bending moment vs embedded pile length

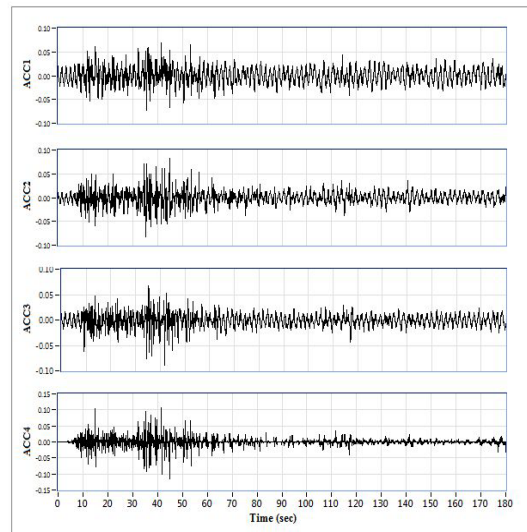
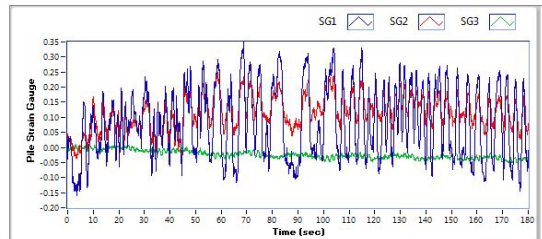
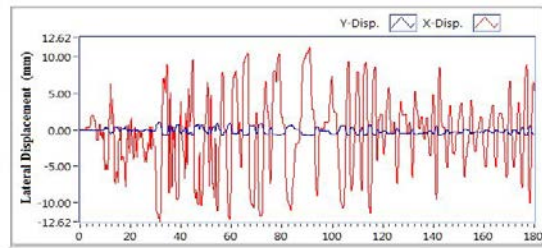
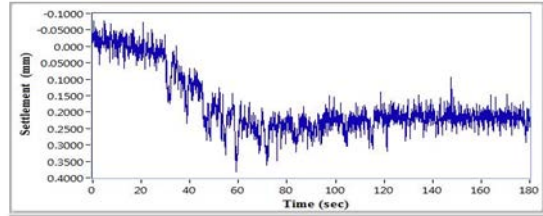
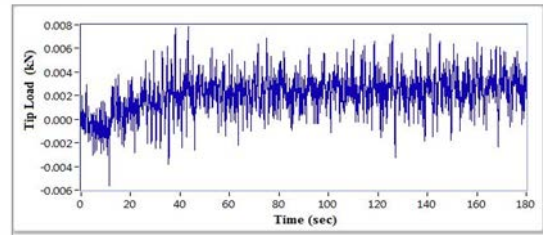


Fig.8. Results of single pile with Nelton geogrid (200×200 mm)

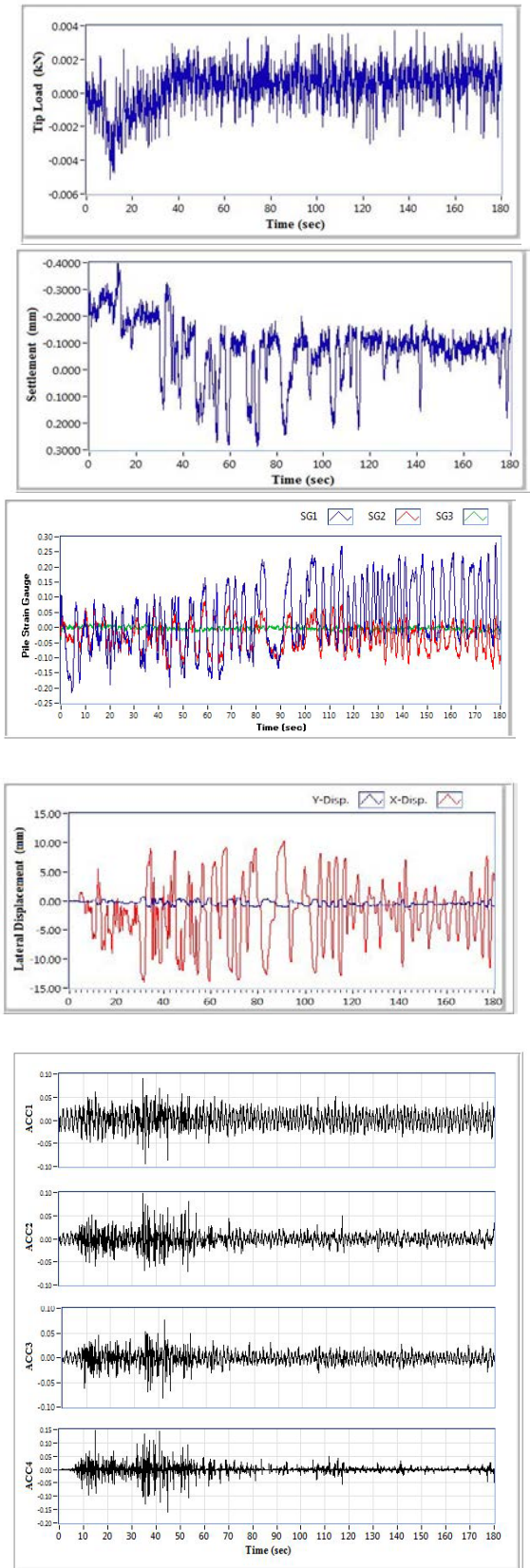


Fig.9. Results of single pile with SQ12 geogrid (200×200 mm)

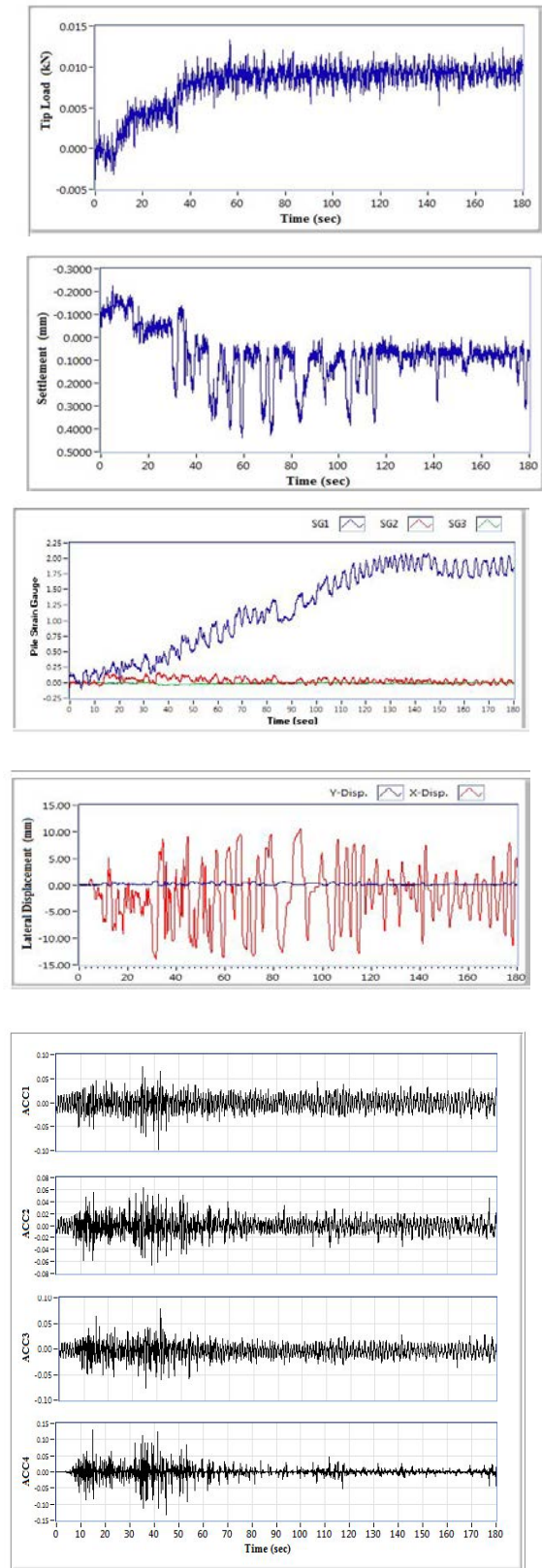


Fig.10. Results of single pile with Tensar geogrid (700×700 mm)

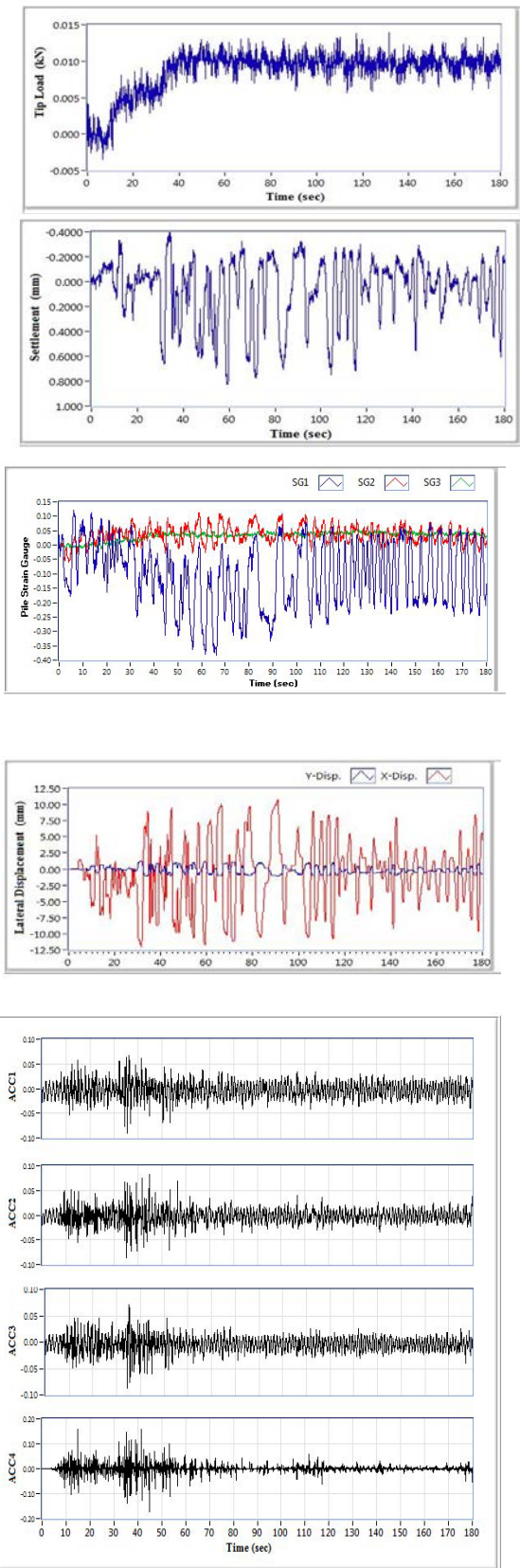


Fig.11. Results of single pile with Nelton geogrid (700×700 mm)

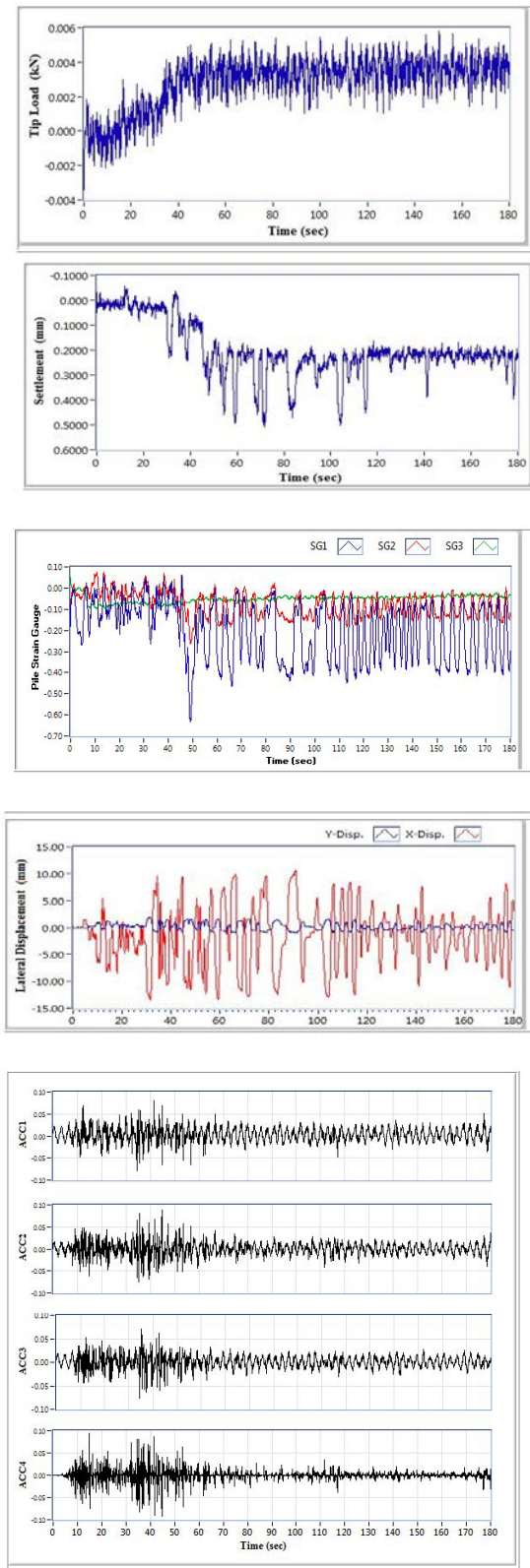


Fig.12. Results of single pile with SQ12 geogrid (700×700 mm)

Figures 8 to 12 show the dynamic time of Halabjah earthquake with accelerations, settlement, tip load, horizontal displacement in two directions and the base shaking. Using reinforcement in soil would control and

decrease the vertical settlement. The reinforcement can contribute to increasing the bearing capacity of the pile may be due to changing in the geometry of the collapse pattern.

It was found from these figures that Tensar geogrid gives a better reduction in the horizontal displacement ratio (the difference between the horizontal displacement without and with geogrid relative to the horizontal displacement without geogrid) reach to 24% because it contains the maximum stiffness than other types. It was found from the results that geogrid participate in the pile in lifting weights then decrease the tip load.

4.1 Effect of Adding Geogrid to Piles on the Pore Water Pressure (P.W.P) Values

Figure 5 illustrates the locations of pore water pressure transducers used. Three saturated tests were used to calculate the pore water pressure values in loose sand under Halabjah earthquake on single pile (with and without geogrid). During horizontal shaking, total and excess pore water pressure generated at the soil bed is measured and recorded using pore water pressure transducers manufactured by “Tokyo Sokki Kenkyujo Co. Ltd, Japan” type KPE-200KPA.. At the pile tip, the maximum pore water pressures typically developed because the ground shaking is large.

The initial liquefaction occurs when the excess pore water pressure ratio $r_u = 1.0$, where $r_u = (\Delta u / \sigma')$, Δu is the increase in pore water pressure and σ' is the effective stress, Saizhao and Chen [9-11]. The pore water pressure accumulated slowly as the acceleration amplitude increased and after 51 seconds, the maximum pore water pressure ratio (r_u) reached 1.04 at the shallow soil depth in the test of the single pile without using geogrid. Liquefaction was observed after 75 seconds from the initiation of shaking, while (r_u) at the middle and bottom depth reaches (0.81 and 0.68) respectively. Then the generated pore water pressure starts to dissipate at 80 second and leveled at 200 second to the initial pore water pressure value.

It is seem clearly from the results of Fig.13 that all the tests would subjected to liquefaction under Halabjah earthquake in the first shallow layer with and without using geogrid. but when using geogrid the excess pore pressure (u_1) decreases in a ratio 17% and 21% when using Nelton CE121 and SQ12 respectively, this happen due to the geogrid work as semi permeable layer which densify the soil around it during shaking. As well as the geogrid layers has increased shear strength of soil and decrease the liquefaction which means that the liquefaction resistance of sand increases due to addition of geogrid layers, Mittal and Chauhan[12-13]. Fig.13 shows the variation of pore water pressure with time, the initial pore water pressure before shaking were recorded as 0.858, 3.432 and 7.722 kN/m² respectively. For unreinforced sand the maximum pore pressure ratio (r_u) recorded in the three

depths was ($r_{u1}=1.04$, $r_{u2}= 0.81$ and $r_{u3}=0.68$), for reinforced sand with Nelton CE121 ($r_{u1}=1.0$, $r_{u2}= 0.70$ and $r_{u3}=0.68$) and for reinforced sand with SQ12 ($r_{u1}=1.02$, $r_{u2}= 0.84$ and $r_{u3}=0.54$). Mokhtar [9] showed that when acceleration higher than 0.10g, full liquefaction could take place ($r_u = 1.0$), then no lateral resistance from the upper liquefied loose sand layer. The results show liquefaction occurs in the surface layer under Halabjah earthquake with and without geogrid.

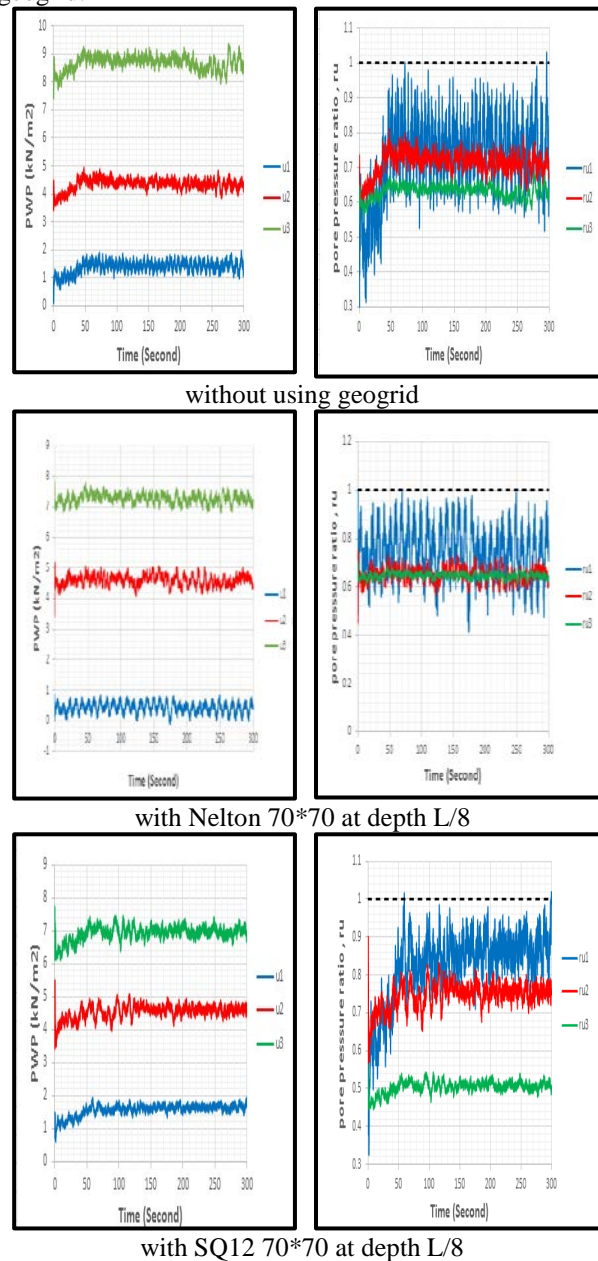


Fig.13. Excess pore water pressure with time in loose sand under Halabjah earthquake

5. CONCLUSIONS

1. There is a relation between peak ground acceleration and soil depth in single pile. The reduction in peak ground acceleration with Nelton CE121

geogrid is greater than without geogrid and it increases with increasing pile number. Adding geogrid will reduce the bending moment values of pile in dry sand while it increased in saturated sand, the bending moment values behave as a cantilever since the highest value is located at the pile head and lowest linearly towards the pile tip. Nelton CE121 (700×700 mm) considered the best type in reduction the bending moment ratio by about 50%, 83% and 60% respectively along the pile length.

2. Adding geogrid to the soil will reduce the settlement. The settlement of pile is effected with position inside a group, where the values in the first row are greater than those in the second row. Nelton CE121 give the better choice in reducing the settlement, the reduction in settlement ratio reaches 76 %. The settlement ratio for pile group reaches to be 33.33 and 37.5% for 2 and 4 pile groups respectively. The settlement in saturated soil is greater than settlement in dry soil for single pile and pile groups. The settlement ratio for single pile in saturated loose soil is 34.2%. In addition increasing the dimensions of the geogrid mesh will reduce the vertical displacement when using geogrid.

3. Adding geogrid will decrease the horizontal displacement of the pile. Tensar geogrid (700×700) mm gives a better reduction in the horizontal displacement ratio reach (24%). Finally in saturated soils using geogrid has insignificant influence on the horizontal displacement ratio and the horizontal displacement ratio for pile groups estimated to be 6% and 12% for 2 and 4 pile groups respectively.

4. Adding geogrid will reduce the tip load of the piles, also the tip load increased with an increasing number of piles and location of piles.

5. Adding geogrid with the pile foundation will reduce the pore water pressure then reduce the occurrence of the phenomena of liquefaction. The excess pore pressure (u_1) decreases in a ratio to 17% and 21% when using Nelton CE121 and SQ12 respectively.

6. REFERENCES

- [1] Taha, A.M. (2014). "Static and Seismic Performance of Geosynthetics-strengthened Pile Foundations", Ph.D. Thesis, Western Ontario University.
- [2] Zanzinger, H., Gartung, E. and LGA (2002). "Performance of a Geogrid Reinforced Railway Embankment on Piles", Geosynthetics – 7th ICG, Nuremberg, Germany.
- [3] ASTM D422. (2007). "Standard Test Method for Practice-Size Analysis of Soils". American Society for Testing and Materials.
- [4] Al-Sammaray, M.M.A. (2018). "Experimental and Numerical Liquefaction Analysis of Layered Sand Soil Under Shallow Spread Footing", Ph.D. Thesis, Department of Civil Engineering, Al-Nahrain University, Baghdad, Iraq.
- [5] Fakhraldin, M.K. (2013). "Properties Measurements and Applications of Some Geogrids in Sand", Ph.D. Thesis, Department of Civil Engineering, Al-Nahrain University, Baghdad, Iraq.
- [6] Al-Tameemi, S.M.K. (2018). "Experimental and Numerical Study on the Effect of Liquefaction Potential of Piles in Sandy Layered Soil under Earthquake Loading", Ph.D. Thesis, Department of Civil Engineering, Al-Nahrain University, Baghdad, Iraq.
- [7] ASTM D845. (2014). "Standard Test Methods for Specific Gravity of Soil Solids by Water Pycnometer". American Society for Testing and Materials.
- [8] Hansen, J. B., (1970). "A Revised and Extended Formula for Bearing Capacity", Bulletin of the Danish Geotechnical Institute, Vol.28, pp. 5-11.
- [9] BS 1377. (1967). "Methods of Test for Soils for Civil Engineering Purposes: Chemical and Electro-Chemical Tests". British Standard Institution.
- [10] ASTM D4767. (2011). "Standard Test Method for Consolidation Undrained Triaxial Compression Test for Cohesive Soils". American Society for Testing and Materials.
- [11] Saizhao DU and Siau C. CHIAN. (2015). " Excess Pore Pressure Generation in Sand Under Non-Uniform Strain Amplitudes", 6th International Conference on Earthquake Geotechnical Engineering 1-4 November, Christchurch, New Zealand.
- [12] Mittal, S., and Chauhan, R., (2013). "Liquefaction behavior of reinforced saturated sand under dynamic conditions", International Journal of Geotechnical Engineering .
- [13] Mokhtar, A.S.A., Abdel-Motaal, M.A., Wahidy, M.M. (2014). "Lateral Displacement and Pile Instability Due to Soil Liquefaction using Numerical Model", Ain Shams Engineering Journal, Vol.5, No, PP: 1019–1032, Egypt.

Copyright © Int. J. of GEOMATE. All rights reserved, including the making of copies unless permission is obtained from the copyright proprietors.
